ISTITUTO NAZIONALE DI FISICA NUCLEARE
Laboratori Nazionali di Frascati

FRASCATI PHYSICS SERIES

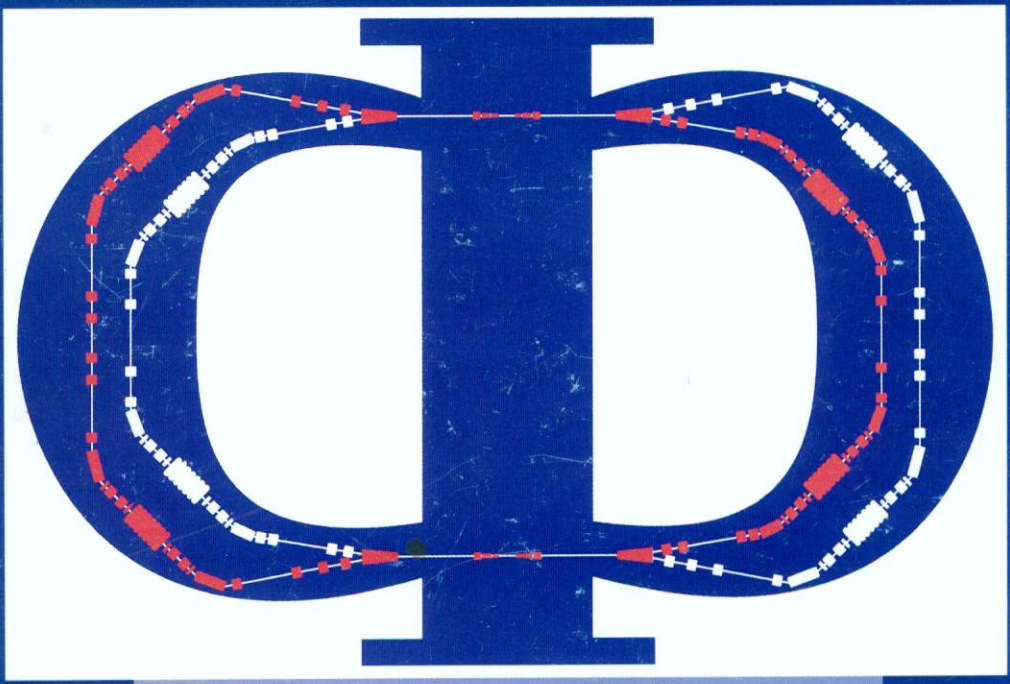

WORKSHOP ON PHYSICS AND DETECTORS FOR DAΦNE '95

Editors
R. Baldini, F. Bossi, G. Capon, G. Pancheri

RECENT RESULTS OF THE ϕ-MESON STUDY WITH CMD-2 AT VEPP-2M AND RELEVANCE TO FUTURE CP,CPT ϕ FACTORY STUDIES

E. P. Solodov*

Budker Institute of Nuclear Physics, Novosibirsk, 630090, Russia

ABSTRACT

The general purpose detector CMD-2 is taking data at the e^+e^- collider VEPP-2M at Novosibirsk, with the luminosity $\approx 5. \times 10^{30} cm^{-2}s^{-1}$. Data from $\approx 1500 nb^{-1}$ of integrated luminosity around 1.02 GeV have been collected (about 1.7×10^6 of ϕ's were produced) and preliminary analyzed. We present progress on study of ϕ-meson and K_SK_L system:

a) the measurement of the ϕ-meson parameters;

b) the search for the rare decays of ϕ. The new upper limits $B(\phi \to \eta'\gamma) < 2.4 \times 10^{-4}$, $B(\phi \to \pi^+\pi^-\pi^+\pi^-) < 1.0 \times 10^{-4}$ and $B(\phi \to f_0\gamma) < 8 \times 10^{-4}$ have been obtained;

c) the study of the K_L interactions in the CsI calorimeter.

d) with the help of 32,340 tagged K_S the semi-rare decay of $K_S \to \pi^+\pi^-\gamma$ has been observed with a branching ratio of $(1.82 \pm 0.49) \times 10^{-3}$;

e) the selection of events with K_SK_L coupled decays and interactions. The regeneration cross section of the low momenta K_L was found to be $\sigma_{reg}^{Be} = 63 \pm 19$ mb.

---

[1]CMD-2 collaboration: Akhmetshin R.R., Aksenov G.A., Anashkin E.V., Astakhov V.A., Aulchenko V.M., Baibusinov B.O., Banzarov V.S., Barkov L.M., Baru S.E., Bondar A.E., Chernyak D.V., Danilov V.V., Eidelman S.I., Fedotovitch G.V., Gabyshev N.I., Grebeniuk A.A., Grigoriev D.N., Ivanov P.M., Khazin B.I., Koop I.A., Kuzmin A.S., Logashenko.I.B., Lysenko A.P., Maksimov A.V., Merzlyakov Yu.I., Monitch V.A., Nesterenko I.N., Okhapkin V.S., Perevedentsev E.A., Polunin A.A., Popkov E.V., Pozdeev E.G., Ptitzyn V.I., Purlats T.A., Redin S.I., Root N.I., Ruban A.A., Ryskulov N.M., Shatunov Yu.M., Sher A.E., Shubin M.A., Shwartz B.A., Sidorov V.A., Skrinsky A.N., Smakhtin V.P., Snopkov I.G., Solodov E.P., Sukhanov A.I., Titov V.M., Yudin Yu.V., Zavarzin V.G., Zverev S.G. - BINP,Novosibirsk, 630090, Russia; Brown D.H., Miller J.P., Roberts B.L., Worstell W.A.- Boston University; Thompson J.A., Valine C.M.- University of Pittsburgh; Cushman P.B.- University of Minnesota; Dhawan S.K., Hughes V.W.-Yale University.

1 Introduction

As it was realized at the very early steps of the ϕ-meson studies at the colliding beam machines, $K_S K_L$ pairs ($\approx 34\%$ of all ϕ decays) may be used as a new source for observing CP and CPT violation. These suggestions, including studies of quantum mechanical correlations, were discussed in papers [1], [2] when an electron-positron collider at Novosibirsk VEPP-2M with luminosity $\approx 5 \times 10^{30} cm^{-2} s^{-1}$, was under construction. The coupled decays of the $K_S K_L$ mesons will allow demonstration of the quantum mechanical correlations of the two particle decays (Einstein-Podolosky-Rosen paradox) [3].

The idea of constructing a more intensive source of ϕ mesons has been discussed by many authors [4], [5]. The flux of events at these so-called "ϕ-factories", now under construction [6], [7], will provide an opportunity to make new precise measurements of a possible direct component in the decay of the $K_L \to \pi^+\pi^-, \pi^0\pi^0$ (ϵ'/ϵ), as well as the observation of the CP-violating three pion decays of the K_S for the first time. The study of the oscillations in the joint decay distributions could give an information about real and imaginary parts of any CPT-violating amplitude.

At the VEPP-2M collider at Novosibirsk, which could be consider as a pre ϕ-factory. With the CMD-2 detector we have been proceeding step by step to prepare for work at the ϕ-factory which is under construction here. Studies of upgraded detectors and accelerators are in progress, including an intermediate $\approx 10^{32}$ luminosity collider for investigating the idea of the round beams, an important ingredient in the planned Novosibirsk ϕ-factory project [8], [9].

With the CMD-2 detector the neutral kaons from ϕ decays are under study and the coupled $K_S K_L$ decays have been observed for the first time. The attempt to select the $K_L \to \pi^+\pi^-$ stressed again problems of the semileptonic decay mode background as well as a high level of neutral kaon nuclear interactions including a regeneration of K_L into K_S. The opening of this kinematic region for the neutral kaon interactions study has been an additional argument for the ϕ factories construction, and we anticipate that the results obtained from the data now in hand will be important in planning ϕ-factory detectors and physics strategies.

A possible problem with a measurement of ϵ'/ϵ at the level of 10^{-4} - 10^{-5} would be an admixture of C=+1 into the final state, giving a component of $K_S K_S$ instead of the desired $K_S K_L$. Although efficient experimental cuts can reduce the effects of such an admixture [10, 11], a component as large as 5×10^{-5} of a C=+1 state would give a dominating contribution to the uncertainty of ϵ'/ϵ at the level of the planned ϕ-factory experiments [11]. The contamination from such a C-even K-$\overline{K}$ mode has been estimated by several authors giving generally lower values [4, 12, 13, 14], but there are no experiments confirming these results.

The decay of the ϕ to $f_0\ \gamma$ with f_0 decaying to two kaons is too small to be seen at the VEPP-2M collider and we hope to study the decay of ϕ to $f_0\ \gamma$ with a subsequent decay of the f_0 to two charged pions [15]. The two charged pion decay mode can be related to the two kaon decay and a limit on the C-even two kaon final state may be found. Estimates for the branching ratio of $\phi \to f_0\gamma$ range from a very small to as high as 2.5×10^{-4} [12, 13, 14].

The study of the f_0 is interesting by itself. The 20% decay probability into a two kaon final state seems puzzlingly high incase if f_0 is a member of the strangeness-0 and isospin-0 meson nonet. Various explanations for this large coupling to kaons have been advanced [12, 13, 14, 16], including the idea that f_0 is really made of four quarks, with a "hidden strangeness" component: $(f_0 = s\,\bar{s}(u\,\bar{u} + d\,\bar{d})/\sqrt{2})$, or that it may be a K-$\overline{K}$ molecule. A limit from VEPP-2M will help to distinguish between these different possibilities.

With expected high luminosity at the ϕ-factories the rare decay modes of ϕ can be measured with high accuracy. For example, a measurement of the $B(\phi \to \eta'\gamma)$ would give an important information about quark structure of light mesons and possible contributions from gluonium states (if any). Our new data obtained with the present statistic already improve upper limit for this process, as well as for $\phi \to \pi^+\pi^-\pi^+\pi^-$ and $\phi \to f_0\gamma$.

The analisys of the CMD-2 data is in progress and we expect new results in the ϕ-meson study.

2 The CMD-2 Detector And Data Sample

The CMD-2 detector has been described in more details elswhere [2, 17]. The CsI barrel calorimeter with 6x6x15 cm crystal size is placed outside a 0.4 r.l. superconducting solenoid with a 1 Tesla azimuthally symmetric magnetic field. The endcap calorimeter is made of 2.5 x 2.5 x 15 cm BGO crystals and was not installed for the data presented here. The drift chamber inside the solenoid has about 250 μ resolution transverse to the beam and 0.5-0.6 cm longitudinally.

The collected sample of the Bhabha events was used for the calibration and determination of the reconstruction efficiency in the drift chamber and in the calorimeter. A momentum resolution of 6-8% for 500 MeV/c charged particles, and energy resolution of about 10% for gammas in the CsI calorimeter have been obtained.

The luminosity integral collected in 1992-1993 at ϕ was mostly used for the detector study and software development. Not all detector systems were running properly and data peresented here are still preliminary – better detector understanding and better reconstruction programms available now will give results with less

systematic errors.

About 7.2×10^7 triggers were recorded. The total luminosity integral, determined by selection of Bhabha events, was found to be 1500 nb^{-1}.

The largest part of the integrated luminosity ($\approx 1200 nb^{-1}$ in the 14 energy points around ϕ mass) have been collected during the 1993 summer runs and was used for study of rare decay modes of ϕ, coupled decays in the $K_S K_L$ sytem and nuclear interactions of neutral kaons.

3 ϕ-meson parameters

The main branching ratios of the ϕ have been measured using $\approx 300 nb^{-1}$ of integrated luminosity, collected in 1992. It was the first time, when four major decay modes of ϕ were measured in one experiment. The events selection and other details may be found in paper [18]. The following results were obtained:

$$
\begin{aligned}
&m_\phi = 1019.380 \pm 0.034 \pm 0.048 \text{ MeV}, \\
&\Gamma_{tot} = 4.409 \pm 0.086 \pm 0.020 \text{ MeV}, \\
&\sigma(\phi \to K^+K^-) = 1993 \pm 65 \pm 82 \text{ nb}, \\
&\sigma(\phi \to K_S K_L) = 1360 \pm 25 \pm 49 \text{ nb}, \\
&\sigma(\phi \to 3\pi) = 656 \pm 24 \pm 30 \text{ nb}, \\
&\sigma(\phi \to \eta\gamma) = 47.9 \pm 3.5 \pm 3.2 \text{ nb}, \\
&\delta_{\omega-\phi} = (147 \pm 16)^\circ .
\end{aligned}
$$

The first error represents the statistical uncertainty and the second one the systematic uncertainty. The relative phase of $\omega - \phi$ mixing in three pion channel is in a good agreement with the most precise measerement presented in [22] $\delta_\phi = (155 \pm 15)^\circ$. The experimental cross-sections of the ϕ production in the different modes, together with fit functions are shown in Figure 1.

All the major decay modes were simultaneously measured in one experiment and therefore the branching ratios can be obtained as ratios of integrals over excitation curves independently of the width of the ϕ and the uncertainties due to the luminosity measurements:

$$
\begin{aligned}
&\mathrm{B}(\phi \to K^+K^-) = 49.1 \pm 1.2 \ \%, \\
&\mathrm{B}(\phi \to K_S K_L) = 33.5 \pm 1.0 \ \%, \\
&\mathrm{B}(\phi \to 3\pi) = 16.2 \pm 0.8 \ \%, \\
&\mathrm{B}(\phi \to \eta\gamma) = 1.18 \pm 0.11 \ \% .
\end{aligned}
$$

The electron width of the ϕ and its branching ratio to e^+e^- can also be calculated independently and were found to be

$\Gamma_{ee} = 1.27 \pm 0.05$ keV,
$B(\phi \rightarrow ee) = (2.87 \pm 0.09) \times 10^{-4}$.

All results are consistent with the Particle Data Group values [23].

Here we note, that in all parameters systematic errors dominate and using all available statistic will improve these results only after systematic errors study and better detector understanding.

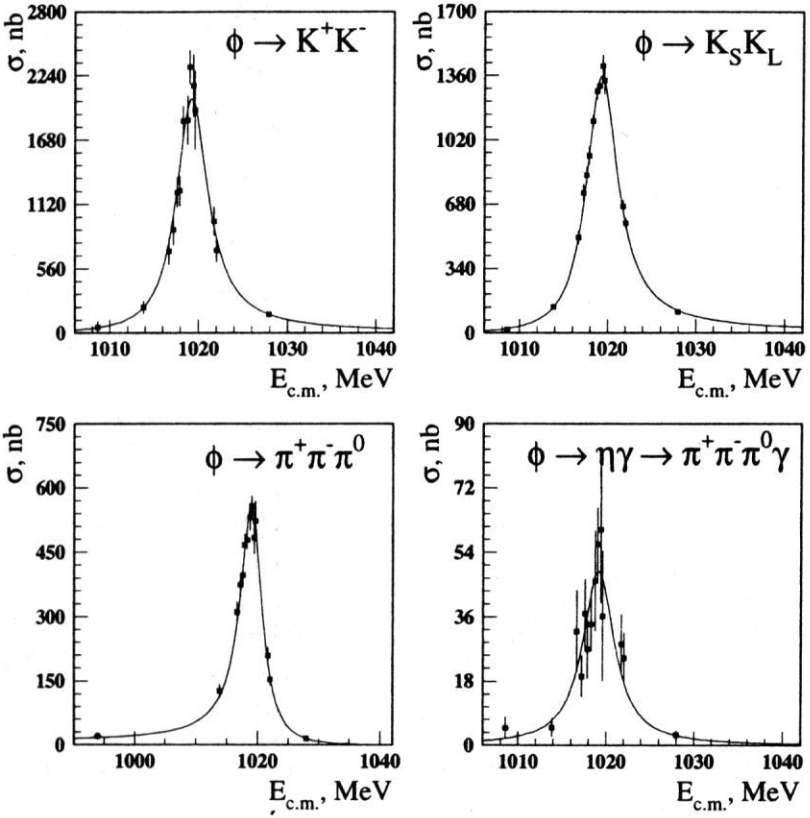

Figure 1: The excitation curves for ϕ-meson in different channels.

4 Study of $\phi \to \eta\gamma$ and Search for $\eta'\gamma$.

The decay of $\phi \to \eta\gamma$ was previosly observed in neutral modes ($\eta \to \gamma\gamma$, $\eta \to 3\pi^0$) only. Detector CMD-2 gives the possibility to study $\phi \to \eta\gamma$ decay in the channel with charged particles, when η decays into $\pi^+\pi^-\pi^0$. So, after $\pi^0 \to \gamma\gamma$ decay, the final state consists of two charged pions and three photons. Two photons in the final state are from π^0, the third one has the maximum energy of all three - 362 MeV at the ϕ-meson peak.

We select $\eta\gamma$ events using the information about momenta and angles from the Drift Chamber for both charged particles and about angle from CsI calorimeter for primary photon under suggestion that other photons are from π^0. The reconstructed invariant mass of 3 pions $M_{\pi^+\pi^-\pi^0}$ is the basic parameter we use to study the decay $\phi \to \eta\gamma$ and the distribution over it should have a peak around M_η = 547.45 MeV.

The distribution over $M_{\pi^+\pi^-\pi^0}$ for all 1993 ϕ-meson data after some simple cuts is presented in Figure 2. These distributions were used to get the numbers of $\eta\gamma$ events for the different beam energies.

The calculated cross-section $\sigma_{e^+e^- \to \phi \to \eta\gamma}$ with fit function is presented in Figure 2. Using the electron width of ϕ from [23] the $Br(\phi \to \eta\gamma)$ was found to be:

$$Br(\phi \to \eta\gamma) = (1.12 \pm 0.06 \pm 0.15)\%$$

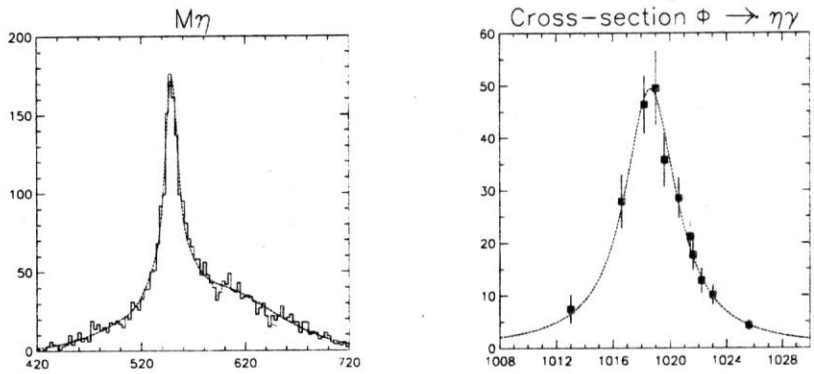

Figure 2: The study of $\phi \to \eta\gamma$: invariant mass $M_{\pi^+\pi^-\pi^0}$; $\phi \to \eta\gamma$ cross-section;

This result is preliminary because the work with efficiency determination is not finished and we hope significally decrease the systematic error.

The decay $\phi \to \eta'\gamma$ was searched in the mode, when η' decays into $\pi^+\pi^-\eta$ and $\eta \to \gamma\gamma$. So, both in $\eta\gamma$ and in $\eta'\gamma$ the final state there are 2 charged particles and

3 photons. The events with all these particles detected were used for the constrained fit.

The scatter plot of the invariant masses for two soft photons M_{23} versus the hardest photon energy ω_1 for the experimental data is presented in the Figure 3.

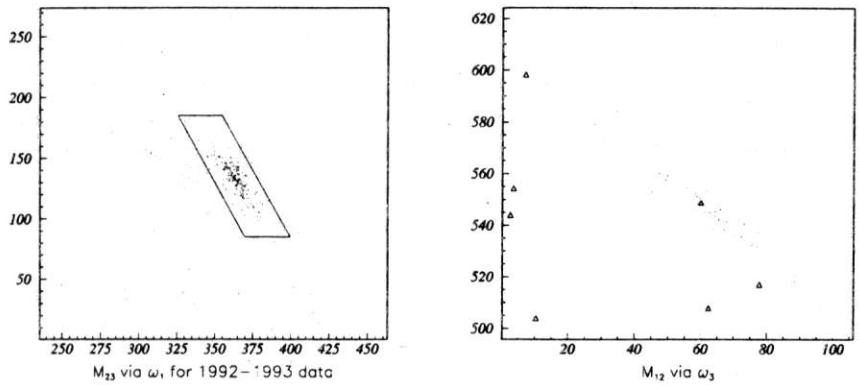

Figure 3: The search for $\phi \to \eta'\gamma$ (1993 data): Invariant mass M_{23} vs. ω_1 after constrained fit. Box shows $\eta\gamma$ cut; Invariant mass M_{12} vs. ω_3 after constrained fit. Dots are simulation, triangles - experiment

The decay into $\eta\gamma$ is the basic background for $\eta'\gamma$. Selecting 481 $\eta\gamma$ events at this plot one can make anti-$\eta\gamma$ cut.

Using this cut the scatter plot of the invariant masses for two hardest photons M_{12} versus the weakest photon energy ω_3 was studied. For $\eta'\gamma$ events M_{12} should be around η mass 547.5 MeV, while ω_3 is monochromatic 60 MeV photon. The Figure 3 presents the result of 1992-1993 data together with simulation of $\phi \to \eta'\gamma$. We have 1 candidate to $\eta'\gamma$ event with 1 event as estimated background. Using for the 90% C.L. upper limit $N_{\eta'\gamma} < 3$ and the ratio:

$$\frac{Br(\phi\to\eta'\gamma)}{Br(\phi\to\eta\gamma)} = \frac{N_{\eta'\gamma}}{N_{\eta\gamma}} \cdot \frac{Br(\eta\to\pi^+\pi^-\pi^0)}{Br(\eta'\to\pi^+\pi^-\eta)} \cdot \frac{Br(\pi^0\to\gamma\gamma)}{Br(\eta\to\gamma\gamma)} \cdot \frac{\varepsilon_{\eta\gamma}}{\varepsilon_{\eta'\gamma}},$$

with the efficiencies obtained from the simulation, $\varepsilon_{\eta\gamma} = 14.4\%$ and $\varepsilon_{\eta'\gamma} = 6.4\%$, the following result has been obtained:

$$Br(\phi \to \eta'\gamma) < 2.4 \cdot 10^{-4}.$$

5 Search for $\phi \to \pi^+\pi^-\pi^+\pi^-$

A sample of 3- and 4-tracks events was used for search for the process $\phi \to \pi^+\pi^-\pi^+\pi^-$. In this sample tracks have to originate from the beam-beam interaction point within 0.5 cm in r-ϕ plane and have at least 9 hits in the Drift Chamber. Total charge have to be ± 1 for 3-tracks events and 0 for 4-tracks events. To suppress background from the two-particle production and cosmic rays with some additional tracks, we reject events with at least two collinear tracks (mutual angle of any pair should be 0.16-3.0 rad in r-ϕ plane).

Even with these selection criteria we have a high background from the main channels of ϕ decaing into 3-tracks events. So, in the search for the process $\phi \to \pi^+\pi^-\pi^+\pi^-$ only 4-tracks events were used. The ratio of 3- and 4-tracks events at the energy points outside ϕ-meson region were used (along with simulation) for evaluation of a detection efficiency which was found to be 0.033 ± 0.012.

The scatter plot E_{tot} vs.P_{tot} for the selected 4-tracks events is shown on the Figure 4a.

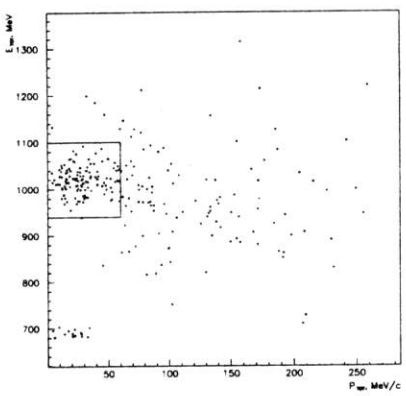

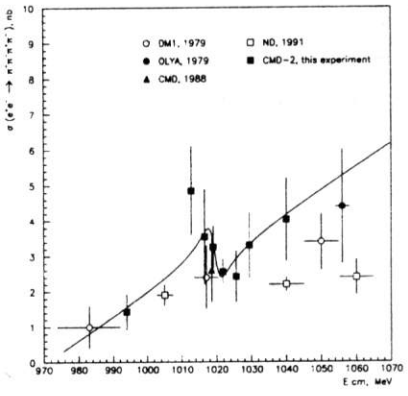

Figure 4: The search for $\phi \to \pi^+\pi^-\pi^+\pi^-$: E_{tot}vs.P_{tot} for 4 - track candidates; cross-section $e^+e^- \to \pi^+\pi^-\pi^+\pi^-$.

Here P_{tot} is the magnitude of the total momentum of 4 charged particles and E_{tot} is their total energy, assuming that all particles are pions. To extract number of events of the process $e^+e^- \to \pi^+\pi^-\pi^+\pi^-$ we apply a simple cut, shown on the Figure 4 by box.

The cross-section vs. energy for the process $e^+e^- \to \pi^+\pi^-\pi^+\pi^-$ is shown on the Figure 4. Only statistical errors are shown. A 4-parameters function which

contains linear background, amplitude and phase of the process $\phi \to \pi^+\pi^-\pi^+\pi^-$ was used for the fitting . Result of the fit is shown on the plot by a smooth line. Using this fit and the uncertanty in the efficiency, one can get

$$Br(\phi \to \pi^+\pi^-\pi^+\pi^-) < 1. \cdot 10^{-4} \text{ for C.L.=90\%}.$$

This preliminary result is about 9 times lower then present upper limit for this process [23]. We plan to perform more simulation to improve both efficiency evaluation and data selection. Also we plan to evaluate and apply radiative corrections which are an order of 5%.

6 Search for $\phi \to f_0\gamma$

In order to extract the resonant contribution associated with the ϕ, two sets of data were used. Energy points at $E_{c.m.}$ from 1016 to 1023.2 MeV with integrated luminosity $660nb^{-1}$ were used for the ϕ region, and points at $E_{c.m.}$ = 996, 1013, 1026, 1030, 1040 MeV with integrated luminosity $440nb^{-1}$ were used for a background estimation (the "non-ϕ" region). The event candidates were selected by a requirement of only two charged tracks and only one photon with energy greater than 20 MeV in the detector. Total energy deposition was required to be less than 600 MeV, average momentum of two charged tracks to be higher than 240 MeV and the radial distance of the found vertex from the interaction region less than 0.15 cm. These cuts removed Bhabha events and charged and neutral kaons from ϕ decays. The requirement that the Z-coordinate of the vertex be within 10 cm at the detector center reduces cosmic ray background by a factorof two.

Each charged track required to have a corresponding cluster in the calorimeter. This requirement reduced the number of pions by about 14%, but avoided nuclear interactions of the pions before the calorimeter with clusters in the wrong place. However split clusters may still be presented.

The main visible background for the studied process is $\phi \to \pi^+\pi^-\pi^0$ decay, when one of the photons from π^0 escapes detection. To reduce this background a constrained fit was used. This fit required total energy and momentum conservation within detector resolutions for the three body decay. For χ^2/d.f. less than 3 only events with these requirements survived. But a three pion background was still presented, when one of the gammas from the π^0 had a very low energy and the event looked like a three body decay. Figure 5 shows the spectrum of the single gammas and the squared missing mass of two charged tracks (taken as pions) vs. detected gamma energy.

In the "ϕ region" data set a broad peak at 200-300 MeV in gamma spec-

trum, also seen as a broad distribution on the scatter plot at $M^2_{\pi^0}$, represents background from the three pion decays. Points concentrated at zero mass and low energy represent events with one gamma. To reduce the three pion and collinear events background, the cuts -15000 $\leq M^2_{inv} \leq$ 15000, $E_\gamma \leq$ 140 MeV and $\Delta\phi \geq 0.03$ rad. were applied. The sample of events, selected with above cuts, still contained about 30% of $e^+e^- \to \mu^+\mu^-\gamma$ events.

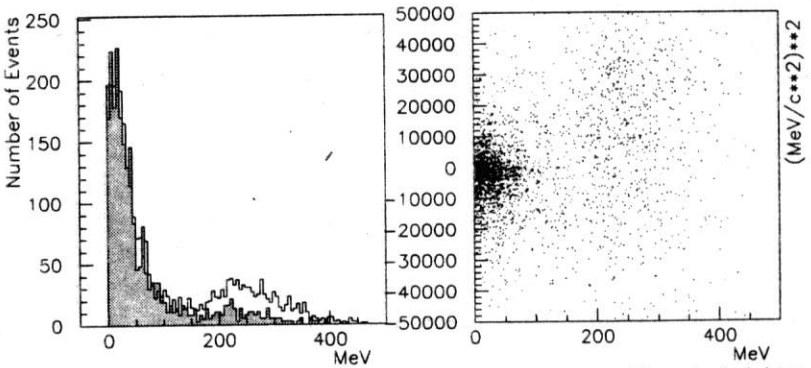

Figure 5: Search for $\phi \to f_0\gamma$: Single gamma spectra. The shaded histogram represents the "not ϕ" region; The squared missing mass vs. photon energy.

The visible cross section of the processes $e^+e^- \to \mu^+\mu^-\gamma + \pi^+\pi^-\gamma$ versus energy is presented in Figure 6a. With the cuts listed above the detection efficiency of these processes, obtained by simulation, was found to be 0.17, leaving 1.7 nb of the visible cross section. The observed 20% difference from average experimental cross section is due to the losses of the the low energy gammas, not correctly described by a simulation. A line shows a theoretical prediction of the cross section including influence of ϕ into photon propagator (vacuum polarization) and f_0 production, according to Achasov four quark model. The total branching ratio of $\phi \to \pi^+\pi^-\gamma$ could be extracted from this interference picture.

The signal from the decay of the $\phi \to f_0\gamma$ should be seen as a 30-40 MeV width structure at 45 MeV in the difference gamma spectra from "ϕ" region and "non-ϕ" region shown in Figure 6b together with the theoretical prediction calculated by Achasov model for the four quark state. With the present statistic only upper limit can be set.

Taking into account the effective number of ϕ's 1.1×10^6 and all inefficiencies described above, the upper limit was found to be

$$B(\phi \to f_0\gamma) \leq 8.0 \times 10^{-4} \; at \; C.L. = 90\%.$$

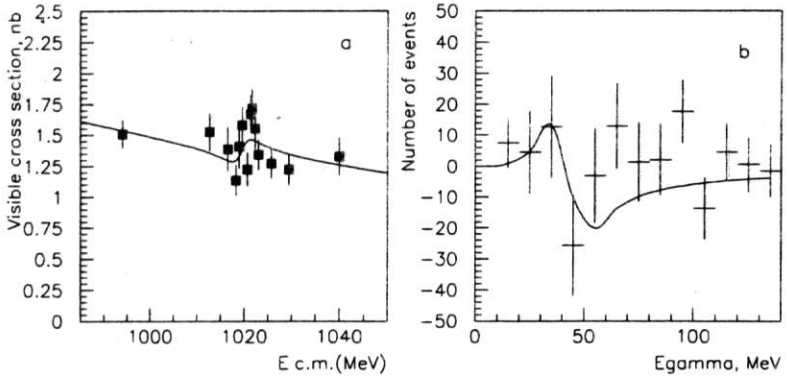

Figure 6: $\phi \to f_0\gamma$ search: a. Visible cross section for $e^+e^- \to \pi^+\pi^-\gamma + \mu^+\mu^-\gamma$ events; b. Normalized difference in photon spectra. A line is a prediction of the four quark model with distructive interference and $B(\phi \to f_0\gamma) = 2.5 \times 10^{-4}$.

7 The K_L nuclear interaction as a tag for K_S rare decay study

K_L candidates are selected by looking at calorimeter clusters opposite a 2-track vertex with an effective mass consistent with that of the kaon. Figure 7a shows the space angle between the predicted missing momentum direction of K_L and the cluster in the calorimeter. Figure 7b shows the energy deposition of the presumed K_L, Figure 7c shows the number of hit crystals, and Figure 7d shows the probability for a K_L to interact, corrected to interaction in the surrounding materials. The clusters from K_L are very broad and in 25 % cases are splitting to 2-4. Simulated distributions are shown shaded. Comparison of the data with the GEANT (with GHEISHA package) simulation shows definite disagreement. The difference is due to compleately incorrect cross sections for the low energy kaons, used by GHEISHA package.

Once the properties of the K_L clusters are understood, one can use the K_L cluster as a "tag" for K_S decays. Figures 8a shows the invariant mass distributions for the events with two charged tracks opposite to K_L clusters.

The constrained fit applied to the decay $K_S \to \pi^+\pi^-$ extracted 32340 events and they were used for a normalization. The rest is shown in Figure 8a by shaded histogramm. In order to search for the $\pi^+\pi^-\gamma$ mode, the sample of events with an acollinearity angle less than 2.4 radians, $M_{inv} \leq 450 MeV/c^2$, and $E_\gamma \geq 50$ MeV is taken.

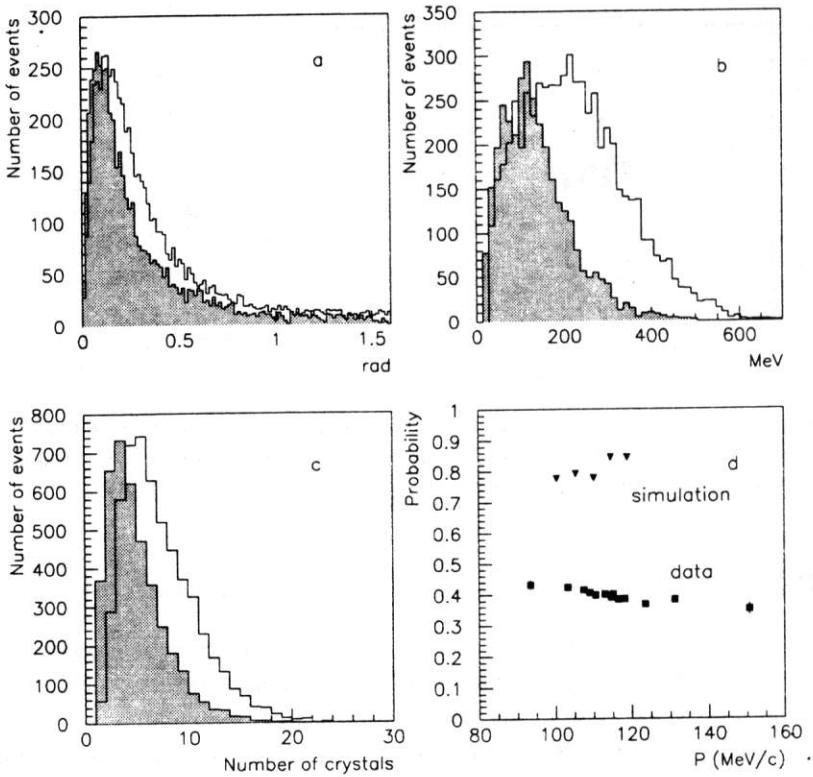

Figure 7: K_L interactions (dashed hists for simulation): a. Space angle between calorimeter cluster and P_{mis}; b. Energy deposition of K_L clusters; c. Number of hit crystals (dashed hists for simulation; d. Probability of K_L interactions in CsI.

Figure 8b shows the missing mass distribution for the two-track vertex, taking the K_S direction from the observed cluster, and the K_S momentum from the known center of mass energy, and assuming $\phi \to K_S K_L$. The 34.5 ± 8.0 events at zero mass, corresponding to the decay $K_S \to \pi^+\pi^-\gamma$ were found after fitting and background subtraction. The simulated ratio of the acceptances for $K_S \to \pi^+\pi^-$ and $K_S \to \pi^+\pi^-\gamma$ was found to be 2.49 ± 0.30, giving a branching ratio $\mathrm{Br}(K_S \to \pi^+\pi^-\gamma) = (1.82 \pm 0.49) \times 10^{-3}$.

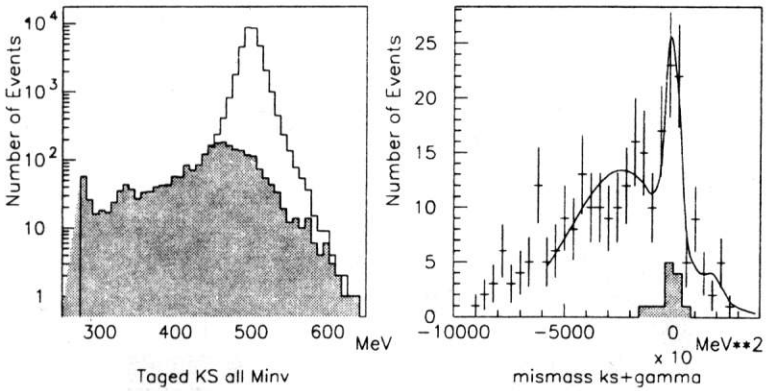

Figure 8: $K_S \to \pi^+\pi^-\gamma$ search: a. Invariant mass for vertecies oposite clusters; Events without K_S decaing to two pions are shown shaded; b. Missing mass in the frame of K_S. Events with real gamma found are shown shaded

8 The K_SK_L coupled decays study

The event candidates were selected from a sample in which two vertices, each of two opposite charged tracks, were seen. The example of this kind of events is shown in Figure 9.

Figure 10a,b show the invariant mass scatterplots of the two charged tracks, assuming that they are pions, vs. missing momentum for the closest to the beam vertex and to the other one. The concentration corresponding to K_S's dominates in the plot 10a and seen in 10b. A two dimensional cuts $470 < M_{inv} < 525$ and $90 < P_{mis} < 130$ with additional requirement to have another reconstructed vertex in the P_{mis} direction within detector resolution, select K_S's in any of the vertex, remaining K_L's in the other. Figure 10c,d show a characteristic M_{inv} and P_{mis} broad distributions, expected from the main 3-body K_L decays in good agreement with the simulation.

Figure 11a shows the distance from the point of origin to the decay point for selected K_S's. The exponential lifelength is seen with correct value 0.58 ± 0.03 cm with vertex position resolution 0.23 cm.

Figure 11b shows the vertex radius for the K_L decays. A loss of efficiency for these events is seen, since the K_L events should be approximately flat in this spatial region corresponding to the very early part of the K_L lifetime. A significant peak with 59 ± 16 events is also seen and is interpreted as the nuclear interactions of

K_L at the 0.077 cm Be vacuum beam pipe.

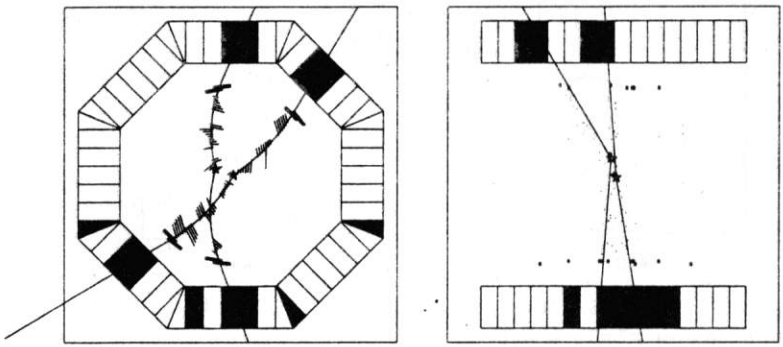

Figure 9: $\phi \rightarrow K_S K_L$ event with coupled decay.

The histogram in Figure 11d shows the events consistent with the two pion decay at the K_L vertices, when additional cut in M_{inv} was applied. With our resolution the suppression of the semileptonic K_L decays by a factor of 20 was expected, and these events dominated at all radii (only 2 CP violating K_L decays were expected with present sample), except beampipe, where 28±6 extra events survived. We interprete these events as regeneration of K_L into K_S.

The rest of the peak events may be explained by Σ and Λ production, when two pions are detected and recoil nucleon is unseen. With the applied M_{inv} cut about 10% of these events may be interpreted as pure two pions decay and should be extracted from the candidates for regenerated events.

Figure 11c shows the projected angle difference between the missing momentum derection and a line, connected K_L vertex with the beam position, for the events concentrated around the beam pipe. Dots with errors show expected distribution for semileptonic decays of K_L, normalized for expected number of these events. A peak at zero angle is seen, supporting expectation about regeneration of K_L into K_S.

Taking into account 10% corrections for DC mylar window and 10% from nuclear interaction processes background, the regeneration cross section is found to be $\sigma_{reg}^{Be} = 63 \pm 19$ mb. A visible nuclear interaction cross section (excluding regeneration) is found to be $\sigma_{nucl}^{Be} = 60 \pm 18$ mb.

The obtained regeneration cross section is in agreement with the calculations, performed in Frascati [24] that gave a value 40 mb for 114 MeV/c long lived kaons.

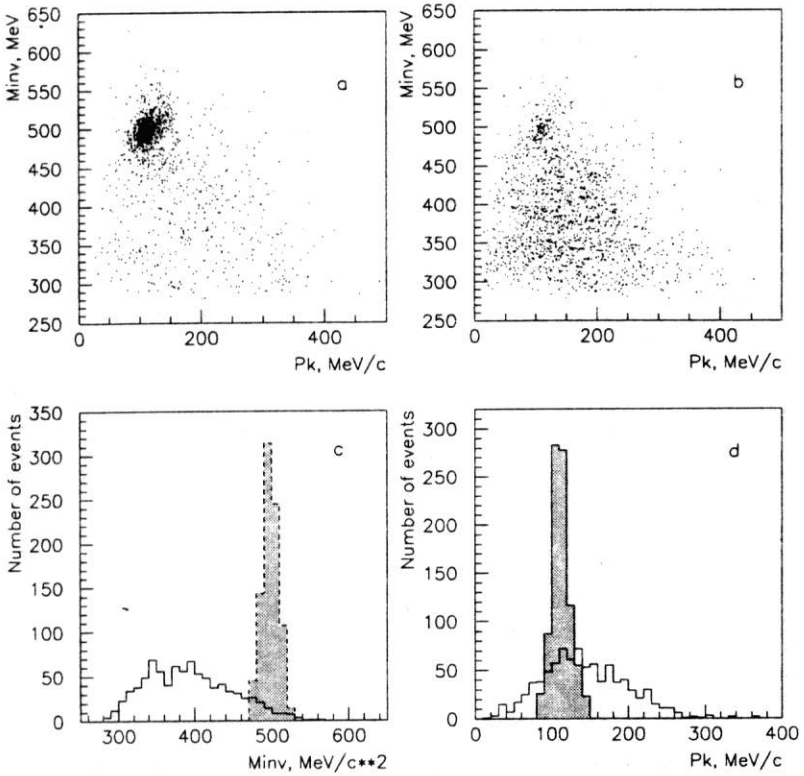

Figure 10: $K_S K_L$ coupled decays study: Invariant mass vs. missing momentum for 1-st (a) and 2-nd (b) vertex; c. Invariant mass for K_L and K_S (shaded) after K_S selection; d. Missing momentum for K_L and K_S (shaded) after K_S selection;

For the total nuclear interaction cross section of neutral kaons one can obtain a value 549±165 mbn, taking into account the ratio 0.21 of hyperon production to all other inelastic processes [25] and 0.52 as ratio of inelastic to elastic cross section [24]. It is also in good agreement with experimental data for higher momenta and calculation, done in [24].

9 Conclusion

The next stage in this work is to process the data with the improved detector resolution and to use all available particle identification information (drift chamber amplitudes, calorimeter energy deposition, and muon detector hits). The detector reconstruction efficiency is under intensive study and will reduce systematic errors in all results presented in this paper. Some other rare decay processes of ϕ are under study.

The presence of a regeneration and nuclear interaction background for the CP-violating decays of K_L will pose an additional background for ϕ factory studies and should be under carefull study.

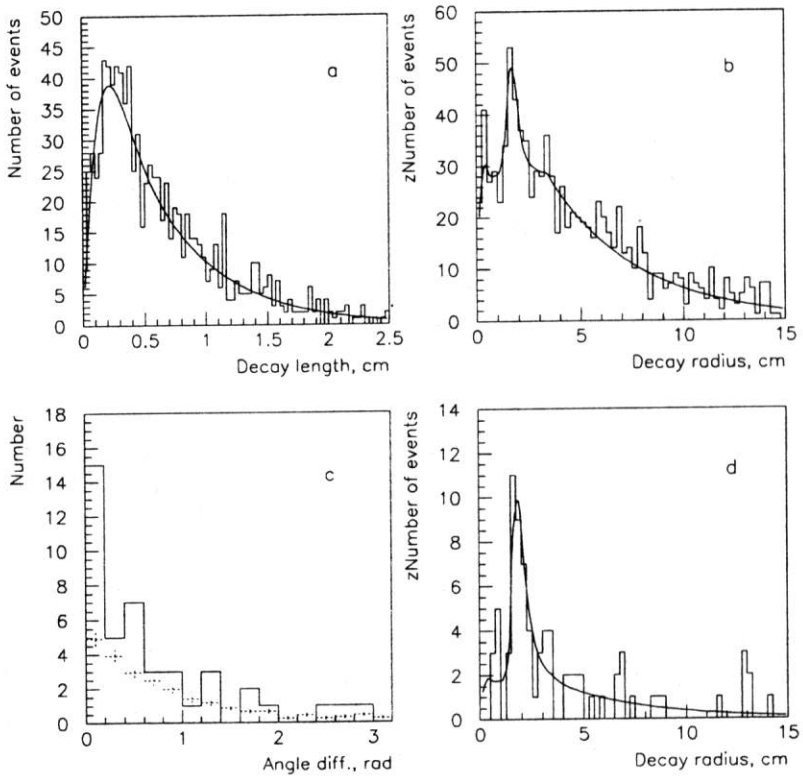

Figure 11: $K_S K_L$ coupled decays study: a. Decay length for K_Ss; b. Decay radius for K_Ls; c. Difference in angle of P_{mis} and vertex-beam line. d. Decay radius for K_Ls after M_{inv} cut; Crosses are from K_L semileptonic decays.

The data taking at ϕ is also planed with at least 10 times more integrated luminosity before reconstruction of VEPP-2M for round beam operation, what promises additional factor of 10 in data sample.

10 Acknowledgements

One of the authors (E.P.Solodov) should thank R. Baldini and A. Michetti for usefull discussion on nuclear interaction study and cooperation in this field.

This work is supported in part by the US Departament of Energy, US National Science Foundation and the International Science Foundation under the grant RPT000.

References

1. V.N.Bayer, ZETFP **17** (1973) 446.

2. G.A.Aksenov et al., Preprint BudkerINP 85-118, Novosibirsk, 1985.

3. P. Eberhard, Contribution to the ϕ Factory Workshop at UCLA, April, 1990.; G.Ghirardi, Proceedings of the Workshop on Physics and Detectors for DAΦNE, Frascati, April, 1991, p.261.

4. J.L. Rosner, I. Dunietz, J. Hauser, Phys. Rev. **D35** (1987) 2166.

5. A partial list of other major contributions includes: A.N.Skrinsky *et al.*, "Novosibirsk ϕ-factory project", F.J. Botella, J. Bernabeu and J. Roldan -Blois CP Violation Conference, FTUV/89-35,IFIC/89-11, May 1989.; G. Barbiellini and C. Santoni, CERN-EP/89-8 and CERN-PPE/90-124; J.A. Thompson, University of Pittsburgh preprint PITT-90-09; contributions by J.A. Thompson, D. Cline, and by C. Buchanan and others to the ϕ Factory Workshop at UCLA, April, 1990.; Y. Fukushima, *et al*,.KEK Preprint 89-159; summary talks by P. Franzini and M. Piccolo and others at the Workshop on Physics and Detectors for DAΦNE, Frascati, April, 1991.

6. A.N.Skrinsky, Proceedings of the Workshop on Physics and Detectors for DAΦNE, Frascati, April, 1991, p. 67.

7. G. Vignola, Proceedings of the Workshop on Physics and Detectors for DAΦNE, Frascati, April, 1991, p. 11.

8. A.N.Filippov et al., Proceedings of the XVth International Conference on High Energy Accelerators, Hamburg, Germany, 1991, World Scientific, V. II, p. 1145.

9. S. Eidelman, E. Solodov, and J. Thompson, Nuclear Physics B (Proceedings Supplement) **24A** (1991) 174.

10. D.Cocolicchio et al., Phys. Lett. **B238** (1990) p.417.

11. P. Franzini, Proceedings of the Workshop on Physics and Detectors for DAΦNE, Frascati, April, 1991.

12. N.N.Achasov & V.N.Ivanchenko, Nuclear Physics **B315**(1989) p.465.

13. S.Nussinov & Tran N. Truong, Phys. Rev. Lett. **63**(1989)1349; A.A. Pivovarov, Soviet Physics - Levedev Institute Reports **9**(1990) 12; N. Paver, contribution to ϕ Factory Workshop at UCLA, April, 1990.; J.L. Lucio & J.Pestieau, Phys. Rev. **D42**(1990)3253; and Oakes, *et al*, Phys. Rev. **D42**(1990).

14. F. Close, Plenary talk at the Workshop on Physics and Detectors for DAΦNE, Frascati, April, 1991, and F.E. Close, Nathan Isgur, and S. Kumano, Nuclear Phys.**B389** (1993) 513.

15. S. Eidelman, J.A.Thompson and C.H.Yang, Proceedings of the Workshop on Physics and Detectors for DAΦNE, Frascati, April 1991, p. 437.

16. The summary talks of L. Maiani and R. Baldini Ferroli and by N.N. Achasov and by M. Pennington at the Workshop on Physics and Detectors for DAΦNE, Frascati, April, 1991.

17. E.V. Anashkin et al., ICFA Instrumentation Bulletin 5 (1988), p.18.

18. Akhmetshin R.R et al., Preprint BudkerINP 95-35, Novosibirsk 1995.

19. J.Lee-Franzini et al., Phys. Lett. **B287** (1992)259.

20. A.Bramon et al., Phys. Lett. **B287**(1992)263.

21. J.Lee-Franzini et al., DAΦNE Physics Handbook, Frascati, 1992, V.II, p.513.

22. Dolinsky et al., Phys. Rep. Vol.202(1991)99.

23. L.Montanet et al., Phys.Rev.**D50**(1994)1173.

24. A. Michetti, Thesises, Roma University, 1993.

25. This value extracted from NUCRIN package.

REVIEW OF RADIATIVE DECAYS STUDY

V.N.Ivanchenko
Budker Institute of Nuclear Physics, 630090, Novosibirsk, Russia

ABSTRACT

Review of experimental studying on radiative decays of light vector mesons is presented. Analisys of magnetic dipole transitions in framework of the constituent quark model is performed.

1 – Introduction

Radiative decays of particles are an important source of information about their structure. The most accurate data on the radiative decays of ρ, ω, ϕ in e^+e^- production were obtained in experiments with the Neutral Detector (ND) at the e^+e^- collider VEPP-2M and was described in detail in the review [1]. Now a real possibility appeared to improve accuracy of radiative decays widths in e^+e^- experiments. After a reconstruction of the VEPP-2M [2] collider in Novosibirsk several runs with the CMD2 detector [3] have been performed and a new SND detector [4] at VEPP-2M has started his first run as well. Moreover, the projects of ϕ-factory DAΦNE in Frascati and ϕ-factory in Novosibirsk are in progress. Thus in this work the experimental status of the radiative decays of light vector mesons and models predictions are discussed from point of view of future experimental program.

2 – Experimental status

After the ND experiment only at this workshop new e^+e^- data from the CMD2 detector at VEPP-2M was reported [5]. Radiative decays of ω were studied for many years in pion production experiments [6, 7, 8] in the reaction $\pi^- p \to \omega n$. The widths of decays $\rho^- \to \pi^-\gamma$, $K^{*\pm} \to K^{\pm}\gamma$, $K^{*0} \to K^0\gamma$ and some other decays were measured using a Primakoff production in hadron-nuclei inelastic scattering [6]. Also one photoproduction experiment was performed [9].

Table 1: Experimental data on radiative decays of vector mesons to $\pi\gamma$.

Decay	Experiment	$\Gamma(keV)$
$\rho^0 \to \pi^0\gamma$	ND [1]	120±30
$\omega \to \pi^0\gamma$		746±50
$\phi \to \pi^0\gamma$		5.5±0.6
$\rho^\pm \to \pi^\pm\gamma$	PDG [6]	68±7
$\omega \to \pi^0\gamma$		717±42
$\phi \to \pi^0\gamma$		5.5±0.6

2.1 $\underline{\rho, \omega, \phi \to \pi\gamma}$

Decays of vector mesons into $\pi^0\gamma$ were studied by ND [1] in the reaction

$$e^+e^- \to \pi^0\gamma \to 3\gamma \tag{1}$$

In this process the recoil photon is monochromatic that enables selection of this reaction. The main background processes are

$$e^+e^- \to 3\gamma \quad (QED), \tag{2}$$

$$e^+e^- \to \phi \to K_S K_L \to neutrals. \tag{3}$$

The process (3) was excluded using selection cryteria for 3γ events. The background from the reaction (2) was calculated and substracted. After that radiative corrections and acceptance corrections were applied. Obtained cross section of the process (1) is shown in fig.1. It was fitted using the vector dominace model (VDM) approximation:

$$\sigma_{e^+e^-\to P\gamma}(s) = \frac{4\pi\alpha^2\omega^3}{s^{3/2}} \left| \sum_V A_V \right|^2, \quad V = \rho, \omega, \phi, \quad s = 4E^2, \quad V = \rho, \omega, \phi,$$

$$A_V = \frac{m_V^2 e^{i\delta_V} \sqrt{\Gamma_{V\to e^+e^-}(s)\Gamma_{V\to P\gamma}(s)}}{m_V^2 - s - i\sqrt{s}\Gamma_V(s)}, \quad P = \pi^0, \eta, \tag{4}$$

where ω is photon energy, δ_V is the relative phase shift, $\delta_\omega = 0$. As a result of the fit two different independent solutions were found according constructive and destructive interference of ρ and ω resonances. The ND data itself doesn't allow to choice one of them but taken into account the results of the Primakoff production experiments [6], in which the process $\rho^\pm \to \pi^\pm\gamma$ was studied, the solution corresponding to destructive interference is excluded on a level of 4 standard deviations. The results and PDG summary are presented in tab.1. One can see that in a e^+e^- experiment obtained width $\Gamma(V \to P\gamma)$ depends on values of m_V, Γ_V, and $\Gamma(V \to e^+e^-)$. Thus to improve accuracy of radiative decay widths these parameters are to be measured with higher accuracy. In this point e^+e^- experiments have real advantage to other type of experiments because beam energy resolution at e^+e^- mashines are much

Table 2: Experimental data on radiative decays of vector mesons to $\eta\gamma$.

Decay	Experiment	$\Gamma(keV)$
$\rho^0 \to \eta\gamma$	ND [1]	62±17
$\omega \to \eta\gamma$		6.1±2.5
$\phi \to \eta\gamma$		55±3
$\omega \to \eta\gamma$	GAM2 [7]	7.0±1.8
$\phi \to \eta\gamma$	CMD2 [5]	54±5
$\phi \to \eta\gamma$		50±7
$\rho \to \eta\gamma$	PDG [6]	57±11
$\omega \to \eta\gamma$		7.0±1.8
$\phi \to \eta\gamma$		56.7±2.7

higher than the widths of resonances. At a ϕ-factory an experimental accuracy in radiative decay widths will be determined both by quality of detectors and by theoretical uncertainty. It is obvious that the model description (4) is to be improved because in it the unitarity is broken. New ways for description of wide resonances are considered. N. N. Achasov and his collaborators have been developing field-theory-inspired approach [10]. M. Benayoun and his collaborators take into account triangle anomalies [11] and include s-dependence of coupling constants. In both cases parameters of resonances are changed significally, branching ratios are less sensitive to model modifications. But additional efforts in this field are necessary.

2.2 $\rho, \omega, \phi \to \eta\gamma$

In e^+e^- experiments decays of vector mesons into $\eta\gamma$ were studied in the following reactions:

$$e^+e^- \to \eta\gamma \to 3\gamma, \tag{5}$$

$$e^+e^- \to \eta\gamma \to 3\pi^0\gamma, \tag{6}$$

$$e^+e^- \to \eta\gamma \to \pi^+\pi^-\pi^0\gamma. \tag{7}$$

High statistic was collected in the ND experiment [1] for the process (5) in the energy region of ϕ and the reaction (6) was used for independent conrol. At the energy region $2E < 1\ GeV$ the reaction (6) was main because of high background for the process (5) from the processes (1) and (2). Cross section of $\eta\gamma$ production is shown in fig.2. Substraction of backgraund were performed. Radiative corrections, the acceptance, and the branching ratios of η decays were taken into account. It is clear from fig.2 that for the $\eta\gamma$ production in energy region of ϕ interference is much smaller than that for the $\pi^0\gamma$ production. The data were fitted using the VDM approximation (4). As in case of $\pi^0\gamma$, two different independent solutions were found according constructive and destructive interference of ρ and ω resonances. Using the data of the GAMS-2000 spectrometer [7] the solution corresponding to destructive interference is excluded on a level of 5 standard deviations. Results are

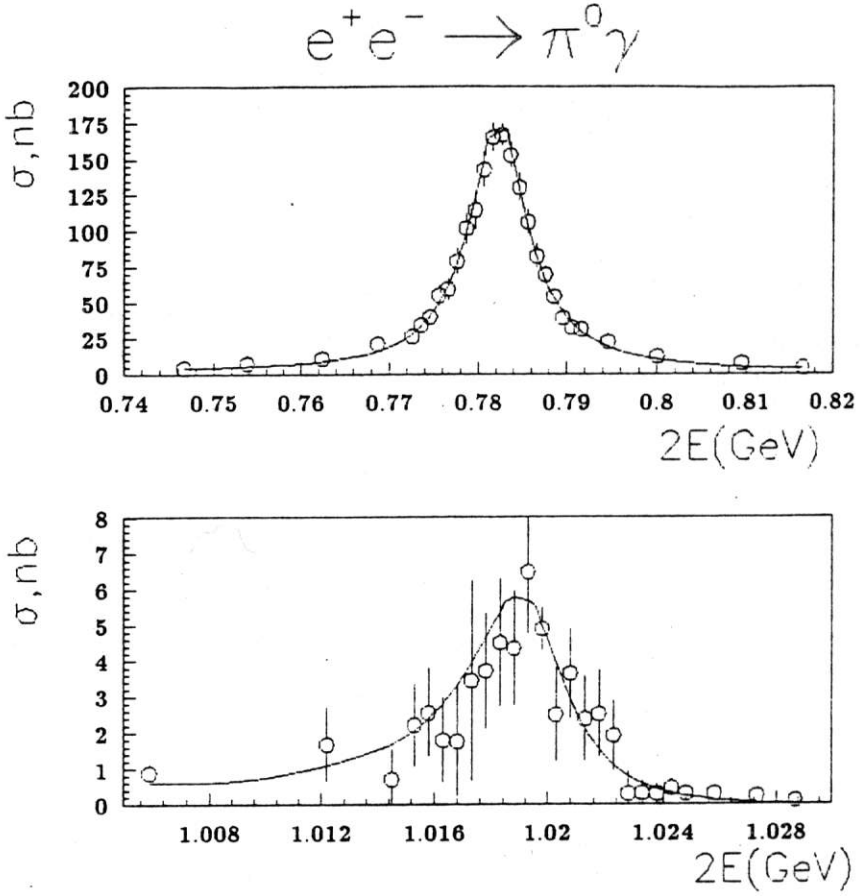

Figure 1: Cross section of the process $e^+e^- \rightarrow \pi^0\gamma$: a) energy region of ρ and ω mesons; b) energy region of ϕ meson; line - the best fit.

Table 3: The data and theory predictions on rare radiative decays of vector mesons.

Decay	Experiment	Branching ratio
$\rho^0 \to \pi^+\pi^-\gamma$	ND [1]	$(0.99 \pm 0.16)\%$
$\omega \to \pi^0\pi^0\gamma$		$< 4 \cdot 10^{-4}$
$\phi \to \pi^0\eta\gamma$		$< 2.5 \cdot 10^{-3}$
$\phi \to a_0(980)\gamma$		$< 5 \cdot 10^{-3}$
$\phi \to \pi^0\pi^0\gamma$		$< 10^{-3}$
$\phi \to f_0(975)\gamma$		$< 2 \cdot 10^{-3}$
$\omega \to \pi^0\pi^0\gamma$	GAMS-2000 [7]	$(7.2 \pm 2.6) \cdot 10^{-5}$
$\phi \to f_0(975)\gamma$	CMD2 [5]	$< 8 \cdot 10^{-4}$
Decay	Theory	Branching ratio
$\omega \to \pi^0\pi^0\gamma$	VDM [1]	$8 \cdot 10{-}5$
$\phi \to \rho\pi \to \pi^0\eta\gamma$	VDM [15]	$0.8 \cdot 10^{-5}$
$\phi \to a_0(980)\gamma \to \pi^0\eta\gamma$	4q [15]	$2 \cdot 10^{-4}$
	qq [15]	$2.4 \cdot 10^{-5}$
	KK molecula [16]	$2.4 \cdot 10^{-5}$
$\phi \to \rho\pi \to \pi\pi\gamma$	VDM [15]	$3 \cdot 10^{-5}$
$\phi \to f_0(975)\gamma \to \pi\pi\gamma$	4q [15]	$2.5 \cdot 10^{-4}$
	qq [15]	$5 \cdot 10^{-5}$
	KK molecula [16]	$5 \cdot 10^{-5}$
	glueball [16]	0

presented in tab.2. Note that in the CMD2 experiment [5] the alternate reaction (7) was stadied. Two independent runs were performed with CMD2 and the results of two independent analisys are presented in tab.2.

2.3 $\rho, \omega, \phi \to \pi\pi\gamma, \pi^0\eta\gamma$

Cross section of the process $e^+e^- \to \omega\pi^0 \to \pi^0\pi^0\gamma$ dominanted for the $\pi^0\pi^0\gamma$ production in the energy region below 1.5 GeV. In the ND experiment [1] the sample of these events is quite clean and there is a good coincidence of the ND data and the data of the DM2 experiment [12]. The CVC calculation [13] shows that the ARGUS data on correspondining τ decay [14] are in agreement with e^+e^- data as well. The shape of this cross section can be described via VDM sum of amplitudes of the ρ resonace and its radial exitations $\rho(1470)$ and $\rho(1700)$. As a result of the fit following value of the coupling constant was found:

$$g_{\rho\omega\pi} = 14.5 \pm 0.4 \pm 0.5, \tag{8}$$

which is in an agreement with that obtained from the width of the ω resonance. Branching ratio of the ρ decay into $\omega\pi^0$ was not presented as a ND result because in the ρ pole this reaction is far below energy threshold and coupling constant is more

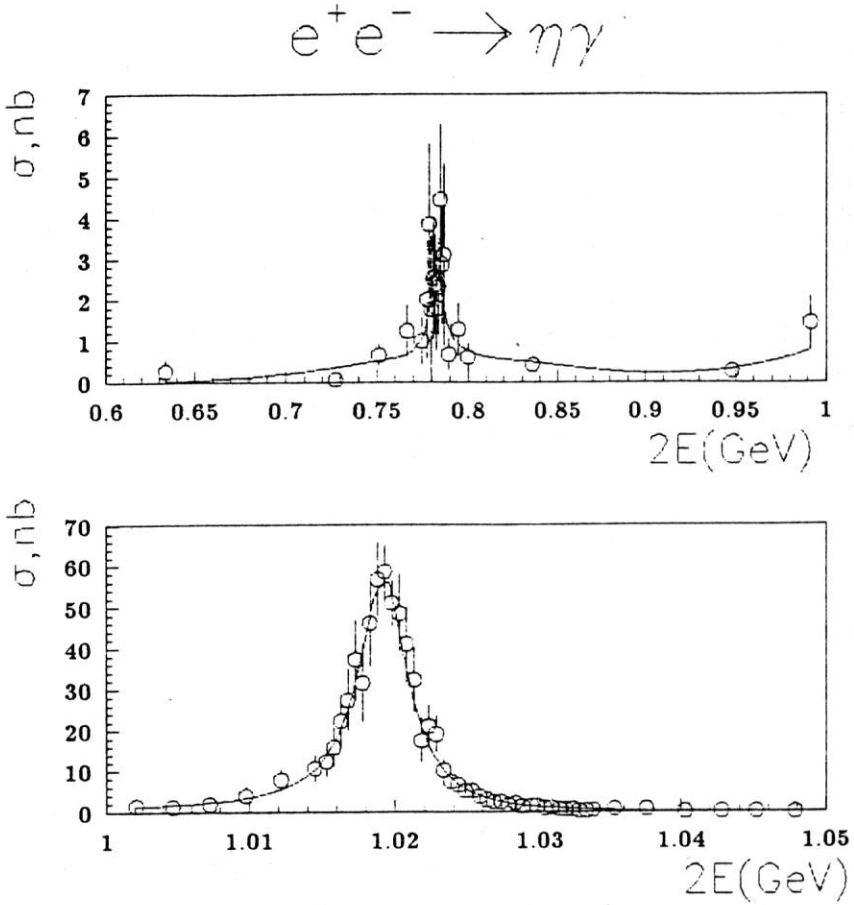

Figure 2: Cross section of the process $e^+e^- \to \eta\gamma$: a) energy region of ρ and ω mesons; b) energy region of ϕ meson; line - the best fit.

adequate value for description of this process. Opposit situation is in $\pi^+\pi^-\gamma$ production. Radiative decay of ρ meson dominates in the pole and the value of branching ratiò are in agreement with the electromagnetic mecanism of the decay [1]. Another mechanisms of $\pi\pi\gamma$ production were not seen until new GAMS-2000 experiment [8] was performed in which the decay mode $\omega \to \pi^0\pi^0\gamma$ was observed. These data and upper limits on another decay modes are shown in tab.3. In tab.3 different model predictions for rare radiative decays of light vector mesons are presented as well. The decay modes

$$\phi \to \pi\pi\gamma, \pi^0\eta\gamma \tag{9}$$

can be realized by two different mechnisms. First one connects with $\rho\pi$ intermediate state and magnetic dipole transition of ρ, so it may be described by the VDM. Second is an electric dipole transition $V \to S\gamma$, where S is scalar state. The processes (9) provide studying of scalars $a_0(980)$ and $f_0(975)$. Structure of these mesons are not clear yet and one of the first tusks for VEPP-2M and DAΦNE is to put light on it. In the ND experiment [1] the backgraund from reactions (3) and (6) did not allow to extract decays (9) of any types. Buy the way, some sygnal was seen in the $\pi^0\eta\gamma$ channel on level of 2 standart deviations and preliminary results of the CMD2 experiment [5] show some evidence for the decay mode $\phi \to f_0(975) \to \pi^+\pi^-\gamma$ as well, but just now only upper limits can be established (tab.3).

3 – Analysis of magnetic dipole transitions

There are a lot of theoretical investigations on magnetic dipole transitions $V \to P\gamma$ and $P \to V\gamma$ in mesons consisted of u, d, s quarks [17, 18] and it is well known that the widths may be expressed as

$$\Gamma(V \to P\gamma) = \frac{4}{3}\pi\omega^3 M_{VP}, \quad \Gamma(P \to V\gamma) = 4\pi\omega^3 M_{VG}, \tag{10}$$

where ω is photon energy, M_{VP} is transition matrix element, which can be written in terms of the magnetic moments of the constituent quarks

$$M_{VP} = I_{VP} \sum_q \beta_q \cdot \mu_q, \quad q = u, d, s. \tag{11}$$

Here I_{VP} is overlap integral of the spatial wave functions of the initial and final states, β_q is a weight factors which can be expressed through the mixing angles α_P and α_V between basis states $s\bar{s}$ and $(u\bar{u} + d\bar{d})/\sqrt{2}$ in the vector and pseudoscalar octets [1]. If one assumes that in all decays under study the overlap integrals are equal, then there are 6 parameters of the model. Three of them are magnetic moments of the constituent quarks, which are well known [6] from the magnetic moments of proton, neutron and Λ baryon

$$\mu_u = 1.852, \quad \mu_d = -0.972, \quad \mu_s = -0.613 \pm 0.004. \tag{12}$$

Since one can suppose some difference between the magnetic moments of s quark in baryons and in mesons the data on decays $V \to P\gamma$ and $P \to V\gamma$ were fitted

with free parameters μ_s, α_P, α_V, I_{VP} (tab.4A). This fit confirms that the magnetic moment of s quark in mesons differs from (12), the value of mixing angle α_P is close to the prediction of the linear mass formula, and the value of α_V is in a good agreement with the quadratic mass formula prediction. On the other hand, within VDM, two-photon widths of the pseudoscalar mesons can be expressed via matrix elements of radiative decays

$$\Gamma(P \to \gamma\gamma) = \frac{3m_P^3}{4\alpha} \left| \sum_V \sqrt{\frac{\Gamma(V \to e^+e^-)}{m_V}} \cdot M_{VP} \right|^2, \quad V = \rho, \omega, \phi. \qquad (13)$$

Comparison of the results of such calculation (tab.4A) with the data shows coincidence for the widths of π^0, $\eta' \to \gamma\gamma$ and disagreement for the $\Gamma(\eta \to \gamma\gamma)$. The fit over all data yields value of $\chi^2/n_D = 46/9$ (tab.4B). Possible improvements of the theory are discussed for many years [18]. There are arguments for taking into account contribution of a glueball state into η' meson. In attempt to check such hypothesis the data were fitted with two additional parameters. First one was the quark-gluon mixture angle α_G. Second was amplitude of η' transition into $\gamma\gamma$ via gluonium M_G, which was added to the sum of amplitudes in the relation (13). χ^2 of this fit (tab.4C) is also poor, but this result is very interesting because we obtained the value of μ_s close to (12) and the value of α_P close to the quadratic mass formula prediction. Therefore the special fit was performed with fixed values μ_s from (12), α_P from quadratic mass formula, and I_{VP} from the value of $\Gamma(\omega \to \pi^0\gamma)$, which has small systematic uncertainty. The results of this calculation show (tab.4D) that practically for all decays there is good agreement between the data and model predictions. The gluonium contents in η' meson is $(20 \pm 5)\%$.

4 – Discussion

Thus simple phenomenological model including quark-gluon mixing can describe the main part of the data on magnetic dipole transitions, but all balk of data cannot be described simultaneously. Let us discuss the results from tab.4 taking into account future experiments in Novosibirsk and Frascati.

First of all one should mention that fitted value of $\Gamma(\omega \to \pi\gamma)$ depends on the model. Accuracy of this width can be increased up to 1% in the new generation of e^+e^- experiments. It will be limited by experimental systematic errors and by theoretical uncertainty in description of the interference of ρ, ω, and ϕ.

Statistic for the decays $\omega, \rho \to \eta\gamma$ is now very poor and obviously will be increased in new e^+e^- experiments, that will allow to have statistical errors for the decay widths about 10%. For such level of statistics the theoretical uncertainty will be small.

Estimated accuracy for the decay width $\phi \to \eta\gamma$ and $\phi \to \pi^0\gamma$ in the new e^+e^- experiments can be improved to $(1-3)\%$. For this aim studying of all decay modes of η in one experiment will be usefull. Energy resolution in e^+e^- experiments

is much higher than the total width of ϕ, that allows to perform accurate extraction of inputs of ρ and ω amplitude at ϕ energy range and to control the resonance shape.

It should be noted that the widths $\Gamma(K^{*\pm} \to K^{\pm}\gamma)$ and $\Gamma(K^{*0} \to K^{0}\gamma)$ depend only on quarks magnetic moments and overlap integrals and do not depend on mixture angles. Both this widths were measured only in Primakoff production experiments with low energy kaon beams. It seems that new independent experiments will be a good cross checking of the existing data and theoretical predictions.

The calculated value $\Gamma(\phi \to \eta'\gamma)$ is very sensitive to model assumptions and varies from 0.1 keV to 0.5 keV. But at the same time this decay is the most difficult for studying. Only upper limit on its width was placed in the ND experiment [1]. At this conference new upper limit was reported by CMD2 collaboration [5]

$$\Gamma(\phi \to \eta'\gamma) < 1 \ keV, \tag{14}$$

and for observation of the decay additional statistic is requiered.

$\Gamma(\eta \to \gamma\gamma)$ was obtained at colliders in two-photon production and also from Primakoff production at hadron beams. If only two-photon measurements are used for the PDG fit, then the average value is $\Gamma(\eta \to \gamma\gamma) = (0.510 \pm 0.026)$ [6], which is closer to the calculated value in tab.4D.

The value of α_V is in a good agreement with the quadratic mass formula prediction. The value of α_P depends on the model and set of new experiments to study radiative decays with η and η' can provide localization of the α_P.

5 – Conclusion

- New generation of e^+e^- experiments have a good perspective for radiative decays study. For these experiments additional theoretical investigations both on the radiative decays and on processes of the production of several wide resonaces in e^+e^- annihilation are necessary.
- Simple constituent quark model cannot describe all data on radiative widths of mesons consisted of u, d, s quarks. If one takes into account 20% admixture of gluonium into η' meson, then it is possible to describe main part of the data using the quadratic mass formula for mixture angles both for the vector and for the pseudoscalar octets. Widths of the decays $K^{*\pm} \to K^{\pm}\gamma$ and $\eta \to \gamma\gamma$ are in contradiction with such model.
- Width of the decay $\phi \to \eta'\gamma$ is very sensitive to model predictions.
- Electric dipole transitions will be extracted from decays into $\pi\pi\gamma$ and $\pi\eta\gamma$ if corresponding branching ratios are about $10^{-4} - 10^{-5}$. Decays of ϕ into these final states provide search on four quark states or kaonium contributions into $a_0(980)$ and $f_0(975)$ mesons.

Table 4: The data on radiative decays and fitting results.

Decay	PDG, $\Gamma(keV)$	Fitting results, $\Gamma(keV)$			
		A	B	C	D
$\rho \to \pi\gamma$	68±8	60	56	59	66
$\omega \to \pi\gamma$	717±42	652	611	648	717
$\phi \to \pi\gamma$	5.5±0.6	5.8	5.5	5.6	5.8
$\rho \to \eta\gamma$	57±11	54	44	40	45
$\omega \to \eta\gamma$	7.0±1.8	5.3	4.2	3.8	4.3
$\phi \to \eta\gamma$	57±3	57	59	61	64
$K^{*0} \to K^0\gamma$	116±10	131	116	114	124
$K^{*\pm} \to K^\pm\gamma$	50±5	55	56	66	75
$\eta' \to \rho\gamma$	59±6	59	71	60	61
$\eta' \to \omega\gamma$	5.9±0.8	6.1	6.9	5.6	5.6
$\phi \to \eta'\gamma$	< 1.7	0.45	0.31	0.15	0.15
$\pi^0 \to \gamma\gamma$	$(7.5\pm0.3)\cdot10^{-3}$	$6.8\cdot10^{-3}$	$6.4\cdot10^{-3}$	$6.7\cdot10^{-3}$	$7.5\cdot10^{-3}$
$\eta \to \gamma\gamma$	0.46±0.04	0.78	0.60	0.53	0.60
$\eta' \to \gamma\gamma$	4.3±0.5	4.5	4.9	4.3	4.3
μ_s	-0.613±0.004	-0.74±0.03	-0.69±0.02	-0.63±0.02	-0.613
α_P (deg.)		-55±2	-50±2	-45±2	-45
α_V (deg.)		3.55±0.20	3.6±0.2	3.5±0.2	3.4±0.2
α_G				35±4	38±3

Acknowledgements

The author is grateful to the organizers of the DAΦNE95 for an opportunity to present this talk and to S.I. Serednyakov for fruitful discussions. This work was supported by the International Science Foundation (grant number 4856/2).

References

1. S.I. Dolinsky et al., Physics Reports 202, **99** (1991).
2. V.V. Anashin et al., Preprint INP 84-123, Novosibirsk, 1984.
3. E.V. Anashkin et al., ICFA Instrum. Bull. **5**, 18 (1988); G.A. Aksenov et al., Preprint INP 85-118, Novosibirsk, 1985;
4. S. Serednyakov et al., SND-Detector for VEPP-2M and Φ-factory, in: Proc. Workshop on Physics and Detectors for DAΦNE (ed. G. Pancheri, Frascati, April 9–12, 1991), 605 (Frascati, 1991).
5. E.P. Solodov, this proceeding.
6. Review of Particle Properties, Phys. Rev. D **50**, 1177 (1994).
7. D. Alde et al., Z.Phys. C **61**, 35 (1994).
8. C. Amsler, Light Quark and Gluonium Spectroscopy, in: Proc. XXVII Inter. Conf. on High Energy Physics (ed.P.J. Bussey and I.G. Knowles, Glasgow, Scotland UK, July 20–27, 1994), **1**, 199 (Glasgow, 1994).
9. D.E. Andrews et al., Phys. Rev. Lett. **38**, 198 (1977).
10. N.N. Achasov, S.A. Devyanin and G.N. Shestakov, Sov. Phys. Usp. **142**, 361 (1984); N.N. Achasov et al., Int. Jour. Mod. Phys. A **7**, 3187 (1992); N.N. Achasov and A.A.Kozhevnikov, Particle World **3**, 125 (1993).
11. M. Benayoun et al., Z.Phys. C **58**, 31 (1993).
12. D. Bisello et al., Preprint LAL-91-64, Orsay, 1991.
13. S.I. Eidelman and V.N. Ivanchenko, Nucl. Phys. B (Proc. Suppl.) **40**, 131 (1995).
14. H. Albrecht et al., Phys. Lett. B**174**, 453 (1986).
15. N.N. Achasov and V.N. Ivanchenko, Nucl. Phys. B**315**, 465 (1989).
16. F.E. Close, N. Isgur and S. Kumano, RAL-92-026.
17. P.J. O'Donnell, Rev. Mod. Phys. **53**, 673 (1981); I.S. Sogami and Oh'Yamaguchi, Phys. Rev. Lett. **54**, 2295 (1985); R.C. Verma and M.P. Khanna, Phys. Lett. B **183**, 207 (1987); F. Gilman and R. Kauffman, Phys. Rev. D **36**, 2761 (1987); G. Morpugo, Phys. Rev. D **42**, 1497 (1990).
18. J.L. Rosner, Phys. Rev. D **27**, 1101 (1983); Sh.S. Eremyan and A.E. Nazaryan, Sov. J. Nucl. Phys. **43**, 863 (1986); **45**, 1758(1987); M.L. Nekrasov, Sov. J. Nucl. Phys. **51**, 1140 (1990); M. Benayoun et al., Z.Phys. C **65**, 399 (1995).

Measurement of the $e^+e^- \to \pi^+\pi^-$ Cross Section in the Energy Range between ρ and Φ Mesons

G.V.FEDOTOVICH*
Budker Institute of Nuclear Physics, Novosibirsk, 630090, Russia

ABSTRACT

The general purpose CMD-2 detector at the VEPP-2M collider in Novosibirsk has collected the luminosity integral of $\sim 300\ nb^{-1}$ in the energy range between ρ and Φ mesons. High accuracy measurements of the e^+e^- annihilation cross section in this energy region are required for the muon g-2 experiment at Brookhaven. The data are also important to interpret the fundamental Standard Model parameters known with high accuracy. Preliminary results of data analysis are presented.

1 – Introduction

The data on the cross section $e^+e^- \to \pi^+\pi^-$ in the energy range between ρ and Φ mesons were obtained with the CMD-2 detector [1, 2] at the VEPP-2M collider [3] at Budker Institute of Nuclear Physics in Novosibirsk. The data from the low energy region up to 1400 MeV (maximum energy provided by VEPP-2M) are important both for the search of rare decays of the light vector mesons and for the calculation

[1]CMD-2 collaboration:
R.R.Akhmetshin, G.A.Aksenov, E.V.Anashkin, V.M.Aulchenko, B.O.Baibusinov, V.S.Banzarov, L.M.Barkov, S.E.Baru, A.E.Bondar, D.V.Chernyak, V.V.Danilov, S.I.Eidelman, G.V.Fedotovich, N.I.Gabyshev, A.A.Grebeniuk, D.N.Grigoriev, P.M.Ivanov, B.I.Khazin, I.A.Koop, A.S.Kuzmin, I.B.Logashenko, A.P.Lysenko, A.V.Maksimov, Yu.I.Merzlyakov, V.A.Monich, I.N.Nesterenko, V.S.Okhapkin, E.A.Perevedentsev, A.A.Polunin, E.V.Popkov, E.G.Pozdeev, V.I.Ptitzyn, T.A.Purlatz, S.I.Redin, N.I.Root, A.A.Ruban, N.M.Ryskulov, Yu.M.Shatunov, A.E.Sher, M.A.Shubin, B.A.Shwartz, V.A.Sidorov, A.N.Skrinsky, V.P.Smakhtin, I.G.Snopkov, E.P.Solodov, A.I.Sukhanov, V.M.Titov, Yu.V.Yudin, V.G.Zavarzin, S.G.Zverev - *Budker Institute of Nuclear Physics, Novosibirsk, Russia*; D.H.Brown, J.P.Miller, B.L.Roberts, W.A.Worstell - *Boston University, USA*; J.A.Thompson, C.Valine - *University of Pittsburgh, USA*; S.Dhawan, V.Hughes *Yale University, USA*; P.Cushman *University of Minnesota, USA*

of the dispersion integral that relates the cross section of e^+e^- annihilation into hadrons to the value of the hadronic vacuum polarization. This value plays on important role in the interpretation of the fundamental Standard Model parameters and the evaluation of the anomalous magnetic moment of the muon [4, 5], which will be measured in the E821 experiment at BNL with an extremely high precision of 0.35 ppm. To evaluate the contribution of the hadronic vacuum polarization to the muon g-2 with the same accuracy a systematic error in hadronic cross section should be less than 0.5%, because the value of the total hadronic contribution is equal to 72 $\pm$1.6 ppm [6]. The main part of this contribution comes from the energy range which is provided by the VEPP-2M collider.

2 – Data Analysis

The data discussed in this talk were obtained by scanning the energy region between ϕ and ρ mesons with 10 MeV step. About 10^3 of pion pairs were sampled at every point. The main part of the luminosity integral $\sim$ 300 nb^{-1} was collected during 1994 runs. Using the resonance depolarization technique [7], the beam energy at each point was measured with the accuracy of 10^{-4}. The detector trigger is described in [8]. Events were recorded when:

* at least one track in the Drift Chamber was found by the tracking processor [9]
* the energy deposition in the CsI calorimeter was greater than 20 MeV.

About 20 million events were written on the magnetic tape. For off-line analysis only collinear two track events were selected. The cuts used for this selection are marked by arrows in Fig.1. Events were used in a maximum likelihood function fit with the following global optimization parameters:

* number of electrons N_e
* number of background events N_b
* $\frac{N_\pi}{N_e+N_\mu}$, where N_π - number of pions and N_μ - number of muons.

The ratio N_μ/N_e was fixed from the QED. The likelihood fit used information on the polar angle, longitudinal coordinate of the vertex and energies deposited in the CsI calorimeter. As it is seen from Fig.2 the experimental data are in a good agreement with the fit.

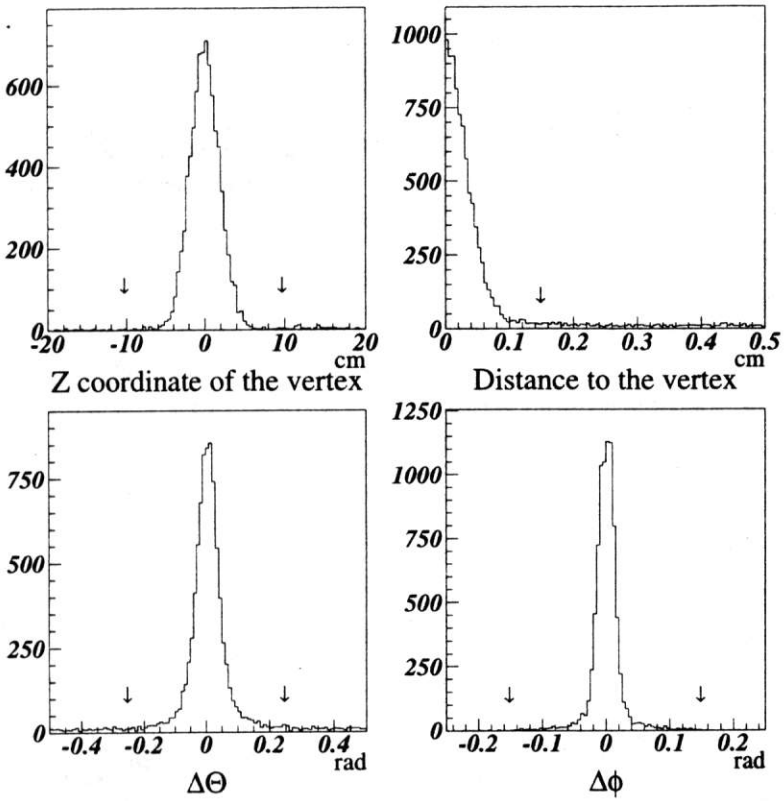

Figure 1: Two track events distributions and cuts imposed to select collinear events.

The ratio $\frac{N_\pi}{N_e+N_\mu}$ allows to express $e^+e^- \to \pi^+\pi^-$ cross section in a simple way:

$$\sigma_\pi = \frac{N_\pi}{N_e + N_\mu} \cdot \frac{\epsilon_e\sigma_e(1+\delta_e) + \epsilon_\mu\sigma_\mu(1+\delta_\mu)}{\epsilon_\pi(1+\delta_\pi)},$$

where ϵ_e, σ_e, δ_e, ϵ_μ, σ_μ, δ_μ, ϵ_π, σ_π, δ_π are detection efficiencies, cross sections and radiative corrections for electrons, muons and pions respectively. Pion formfactor values are presented in Fig.3 along with the results of the previous experiments.

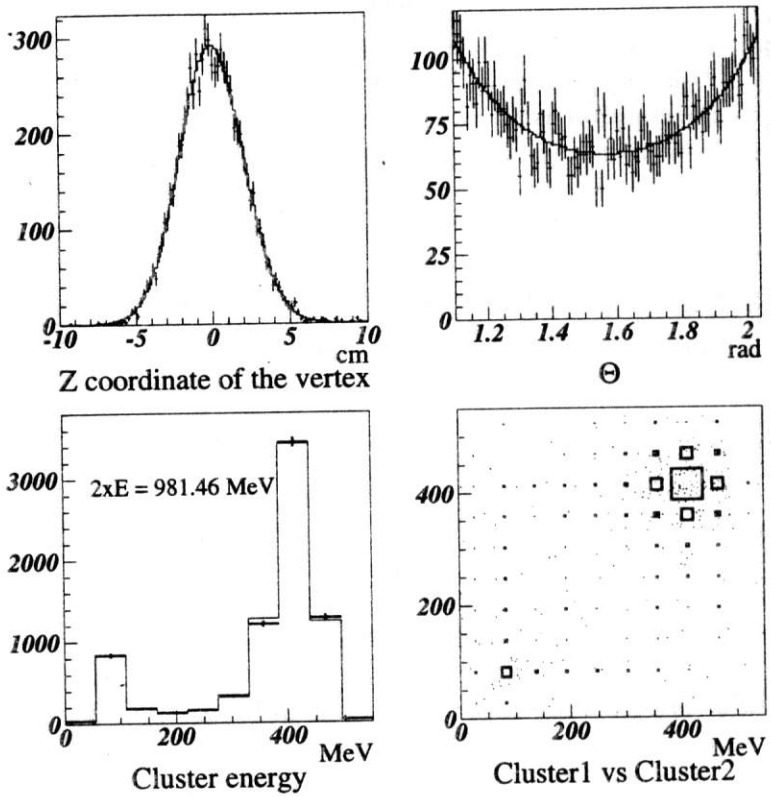

Figure 2: The comparison of the experimental data with a fit.

The statistical error of the $\pi^+\pi^-$ cross section at each energy point is better than 3%. At present the total systematic error is estimated to be $\sim$ 1.5%. The main part of this error comes from the detector solid angle uncertainty $\sim$ 1% and from the calculation of the radiative corrections for Bhabha events [10], which are known with accuracy $\sim$ 1%. Radiative corrections for all other channels of the e^+e^- annihilation into hadrons and muons were calculated with the accuracy about 0.2 - 0.5% [11, 12] which is sufficient for the purposes of the experiment. As an example, we describe very briefly the main idea and approach to calculation of the radiative corrections for the channel $e^+e^- \to \pi^+\pi^-$ in Appendix.

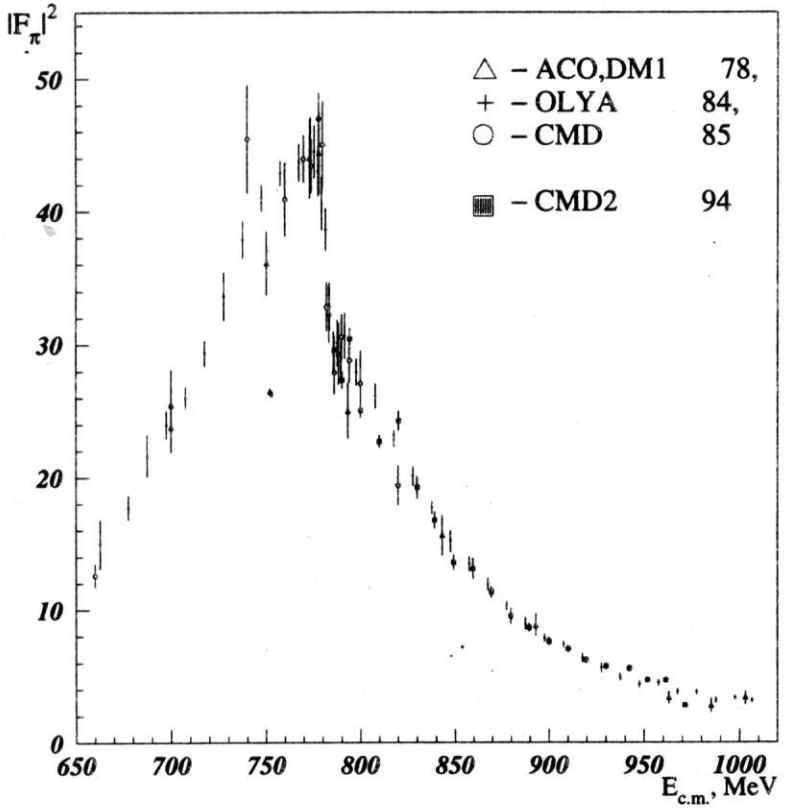

Figure 3: The experimental data for $|F_\pi|^2$.

The further improvement of the Drift Chamber parameters and more accurate calculations of the radiative corrections for Bhabha scattering events would decrease the systematic error to the level of 0.5%.

This work is supported in part by the US Department of Energy, US National Science Foundation and the International Science Foundation under the grant RPT000.

References

1. G.A. Aksenov et al., Preprint INP **85-118**, (Novosibirsk 1985).

2. B.I. Khazin et al., Proc. of the XXVI Int. Conf. on High Energy Physics, **2**, 1876,(1992) (Ed. J.R. Sanford).

3. V.V. Anashin et al., Preprint INP **84-114**, (Novosibirsk 1984).

4. M. Vysotski, Plenary talk, Proc. of the XXVII Int. Conf. on High Energy Physics.

5. Muon g-2 Design Report AGS 821, BNL, July (1992).

6. S. Eidelman and F. Jegerlehner, Preprint PSI-PR **95-01**, (1995).

7. Ya.S. Derbenev et al., Part. Acc. **10**, 177 (1980).

8. E.V. Anashkin et al., Nucl. Instr. Meth. **A323**, 178 (1992).

9. V.M. Aulchenko et al.,Nucl. Instr. and Meth.,**A252**, 299, (1986).

10. F.A. Berends and R. Kleiss, Nucl. Ph., **B228**, 537 (1983).

11. E.A. Kuraev, V.S. Fadin, Soviet Journal of Nuclear Physics,**41**, 466, (1985).

12. E.A. Kuraev al all. Will be published.

13. F.A. Berends and G.J. Komen, Physics Letters, **B63**, 432, (1976).

3 –Appendix

Our technique for the calculation of the radiative corrections is based primarily on two works [11, 12]. The first one gives an accuracy about 0.2% but the cross section is integrated over all final particles kinematics except for the total energy loss and furthermore is valid only for comparatively small energy losses (under 10% of the beam energy). The second one is less accurate (about 0.5%) and assumes that only one photon is emitted but it gives the angle distributions for the final particles, which is important when any selection criteria are applied to the events.

Our procedure for the calculation of the radiative corrections is combined both approaches in the following way: photons with the energy less than ΔE are simulated according to [11] while photons with the energy greater than ΔE are simulated according to [12]. The quantity ΔE is a free parameter and its selection will be discussed later. In order to get a smooth and continuous distributions over final particles kinematics, energy loss for a region under ΔE was assigned to a "hypothetical" single photon having the same angular distributions as follows from [12]. The dependence of the radiative corrections for the channel $e^+e^- \to \pi^+\pi^-$ on

the value of ΔE is shown in Fig.4 under selection criteria (mentioned above in the talk) for the collinear events.

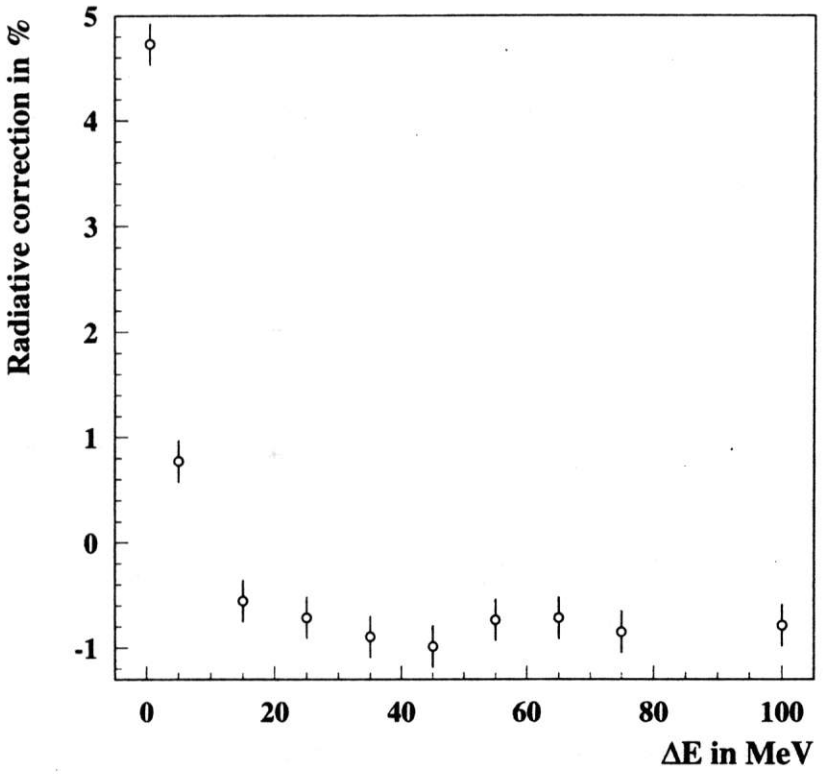

Figure 4: The dependence of the radiative corrections on ΔE for the energy 952 MeV.

One can see that in a wide region of the ΔE values the total cross section does not depend on ΔE with the accuracy of about $0.2 - 0.3\%$.

The possible values of ΔE are limited by the following factors:

* ΔE should not exceed the validity region of [11)]
* ΔE should be large enough for the approach of the single photon to be applicable
* it is desirable to have ΔE as large as possible to use the

better accuracy of [11]

* for large energy losses causing the events rejecting by the selection criteria an approach [12] should be used to take proper account of the final particles kinematic.

Thus the reasonable values of ΔE are limited on both sides and should be somewhere from 20 to 50 MeV depending on the beam energy and the selection criteria of the collinear events.

The expression for the calculation of the radiative corrections for the channel $e^+e^- \to \pi^+\pi^-$ is briefly described below. Calculations of the radiative corrections for the other channels were done in a similar way.

The cross section used for the calculation of the radiative corrections can be expressed as follow:

$$\frac{d\sigma_\pi(S)}{d\Omega_-} = \int_0^\Delta \frac{d\sigma_0(S_1)}{d\Omega_-} \cdot \frac{F(S,x_\gamma)}{|1-\Pi(S_1)|^2} dx_\gamma +$$

$$+\frac{2\alpha}{\pi} \int_\Delta^{X_\gamma{}^{max}} f_{en}(x_\gamma)dx_\gamma \int_{-1}^{1} f_{ang}(Z_\gamma)dZ_\gamma \frac{d\sigma_0(S_1)}{d\Omega_-} \left|\frac{F_\pi(S_1)}{F_\pi{}^{BW}(S_1)}\right|^2 \frac{R(S,Z_-,x_\gamma,Z_\gamma)}{|1-\Pi(S_1)|^2},$$

where

$$\frac{d\sigma_0(S)}{d\Omega_-} = \frac{\alpha^2}{8S}\beta_\pi{}^3(1-Z_-{}^2)$$

- is the Born cross section,

$$f_{en}(x_\gamma) = \frac{1}{x_\gamma(1-x_\gamma)[(1-\frac{S(1-x_\gamma)}{M_\rho{}^2})^2 + \frac{\Gamma_\rho{}^2}{M_\rho{}^2}]}$$

- is a function used for the simulation of the photon energy,

$$f_{ang}(Z_\gamma) = \frac{1}{1-\beta_e{}^2 Z_\gamma{}^2}[1 - \frac{1}{1+\gamma_e{}^2(1-Z_\gamma{}^2)}]$$

- is a function used for the simulation of the polar angle of the photon emitted by the initial particles,

$|F_\pi(S)|^2$ - is the pion formfactor squared,

$\left|F_\pi{}^{BW}(S)\right|^2$ - is the pion formfactor squared in the simplest Breit-Wigner form,

$\Pi(S)$ - is the vacuum polarization due to leptons and hadrons [11, 13],

$F(S,x_\gamma)$ - is the structure function [11],

$$R(S,Z_-,x_\gamma,Z_\gamma) = \frac{1}{|1-\Pi(S_1)|^2} \cdot \frac{1}{\beta_\pi{}^3(1-Z_-{}^2)} \cdot [\frac{\beta_- x_-}{2-x_\gamma(1-cos(\Phi)/\beta_-)}] \cdot |M|^2.$$

The expression in the squared brackets is connected with the phase space of the final particles. $|M|^2$ is the dimensionless square of the matrix element for $e^+e^- \to \pi^+\pi^-$ process from which the main peculiarities ($f_{en}(x_\gamma)$ and $f_{ang}(Z_\gamma)$) are factored out.

$$|M|^2 = [1 + \frac{1}{\gamma_e{}^2(1 - Z_\gamma{}^2)}] \cdot \frac{R_1 + R_2}{1 - x_\gamma},$$

where [12]

$$R_1 = [(2 - x_\gamma)^2 + x_\gamma{}^2 Z_\gamma{}^2](\beta_\pi{}^2 - x_\gamma) - (1 - x_\gamma)[(x_+ - x_-)^2 + (x_+\beta_+ Z_+ - x_-\beta_- Z_-)^2]$$

and

$$R_2 = -\frac{1}{1 + \gamma_e{}^2(1 - Z_\gamma{}^2)}[4(1 - x_\gamma)(\beta_\pi{}^2 - x_\gamma) - (x_+(Z_\gamma + \beta_+ Z_+) - x_-(Z_\gamma + \beta_- Z_-))^2]$$

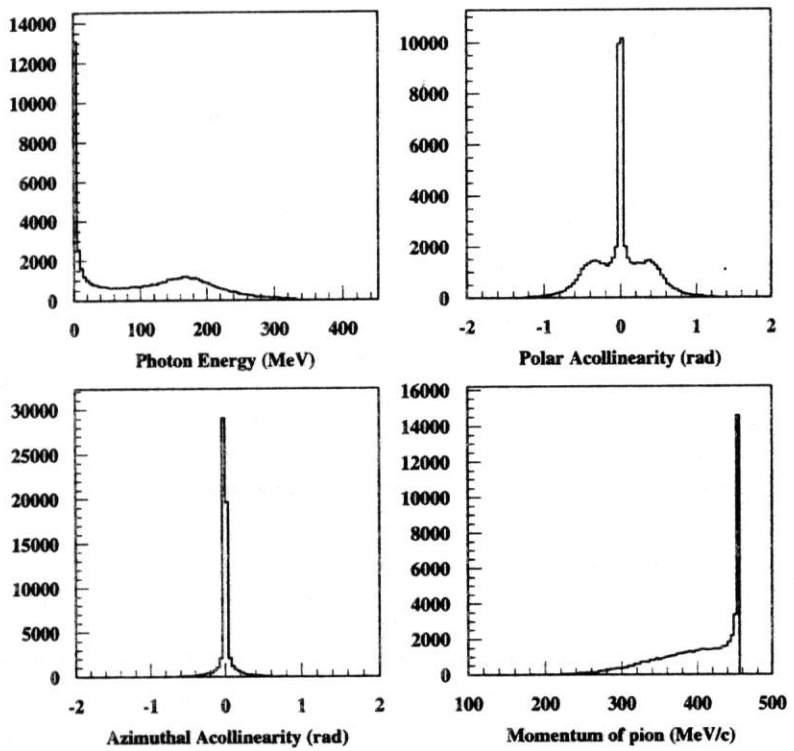

Figure 5: The distributions of the final state particles for the energy 952 MeV.

The following designations were used in the previous expressions: x_+, x_-, x_γ - energies of the final pions and photon divided by E_{beam} respectively; Z_-, Z_+, Z_γ - their polar angles cosines; β_+, β_- - velocities of pions; $S = 4E^2_{beam}$; $S_1 = S(1-x_\gamma)$; $\Delta = \Delta E/E_{beam}$; $\gamma_e = E_{beam}/m_e$; $\beta_e = P_e/E_{beam}$; $\beta_\pi = P_\pi/E_{beam}$; E_{beam} - energy of the electron (positron); P_e - their momenta; m_e and m_π are the electron and pion masses.

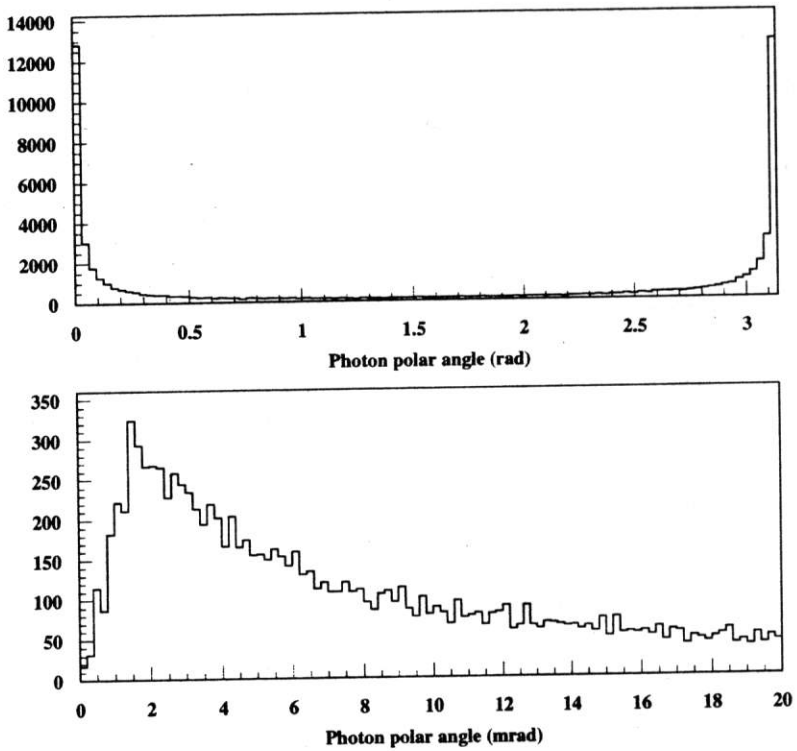

Figure 6: The photons distributions on the polar angle.

The $|M|^2$ is a smooth function that provides a high efficiency of the simulation. For the photons with the energies less than ΔE the efficiency is about 70-80% depending on the c.m.s. energy. For the photons with the energies more than ΔE the efficiency varies from 10 to 60% depending on the c.m.s. energy, reaction channel and selection criteria.

According to expressions described above 50000 events of the $e^+e^- \to \pi^+\pi^-\gamma$ process were simulated at the center of mass energy 952 MeV. Some of the distributions for the final state particles are shown in Fig.5-6. No selection criteria were used except that one of the charged particles should has the angles inside of the solid angle CMD-2 detector. On the first histogram of Fig.5 the energy spectrum of the emitted photons is represented. There is a bump near 160 MeV that corresponds to the dumping to ρ meson resonance. On the second histogram the polar acollinearity between two pions is shown. There are two symmetric bumps around the central peak that also correspond to the dumping to the resonance. On the third histogram the acollinearity between two pions in the azimuthal plane is shown. On the last histogram the momentum spectrum of pions is represented. The long tail can be explained by the emitted hard photons and by the dumping to the resonance. In Fig.6 two distributions over polar angles of the emitted photons are represented. The last one shows a small polar angles region in more details.